3-D KINETICS SIMULATIONS OF THE NRU REACTOR USING THE DONJON CODE

T.C. Leung*, M.D. Atfield* and J. Koclas+

*AECL, Atomic Energy of Canada Ltd, Chalk River Laboratories, Chalk River, ON. K0J 1J0, Canada.
+Institut de génie nucléaire, École Polytechnique de Montréal, 2900 Boulevard Édouard-Montpetit, Montréal, Québec, H3T 1J4, Canada

Abstract

The NRU reactor is highly heterogeneous, heavy-water cooled and moderated, with on-line refuelling capability. It is licensed to operate at a maximum power of 135 MW, with a peak thermal flux of approximately 4.0 x 10^{18} n.m^{-2}.s^{-1}. In support of the safe operation of NRU, three-dimensional kinetics calculations for reactor transients have been performed using the DONJON code. The code was initially designed to perform space-time kinetics calculations for the CANDU® power reactors. This paper describes how the DONJON code can be applied to perform neutronic simulations for the analysis of reactor transients in NRU, and presents calculation results for some transients.

KEYWORDS: Reactor Physics, Research Reactor, 3D Kinetics, Core Simulation, Reactor Transient

1. Introduction

The NRU reactor at the Chalk River Laboratories is a highly heterogeneous, heavy-water cooled and moderated research reactor, with on-line refuelling capability. It is mainly used to produce neutrons for fundamental research, for radioisotope production, and for reactor material and fuel bundle testing for the CANDU power reactor development program. It has a peak thermal flux of 4.0 x 10^{18} n.m^{-2}.s^{-1}, and is licensed to operate at a maximum power of 135 MW [1]. Figure 1 shows a NRU core lattice, with rows (1 to 31) and 18 columns (A to S, with no column "I"). The hexagonal lattice pitch between adjacent rod assemblies is 19.685 cm.

Three-dimensional kinetics calculations for reactor transients have been performed in support of the safe operation of NRU. This paper describes the detailed three-dimensional modeling of NRU for kinetics calculations using the DONJON code [2], and presents calculation results for some transients.

2. Modeling the NRU Reactor Using DONJON

The DONJON code was developed by the staff of Ecole Polytechnique of Montreal in the early 1990's using diffusion theory. It is a static and dynamic 3D multi-group code, with

---

CANDU® is a registered trademark of Atomic Energy of Canada Limited (AECL).

Figure 1: The NRU Core Lattice

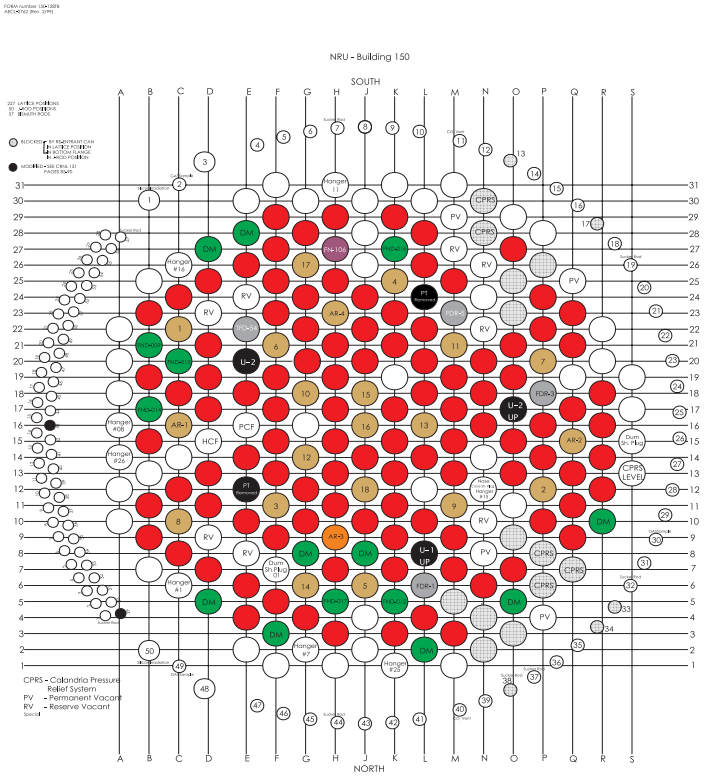

a variety of spatial discretization techniques, including finite differences and higher order finite element methods. The code was later modified to include calculations using the mesh-centred finite-differences and the analytic-nodal method [3,4]. The modified code was designed to perform space-time kinetics calculations for the CANDU power reactors. It has been applied successfully for the analyses of Reactor Regulating System (RRS) transients, xenon transients, reactivity device movements and large LOCA in CANDU-6 reactors.

The NRU core that was used for the analysis consisted of 85 driver fuel rods with axial burnup variation, 12 Mo-99 production rods, 3 loop fuel strings, 22 cobalt absorber rods, with the remaining sites being heavy water. The modeling of NRU was performed in 3D Cartesian geometry for 301 sites. For the NRU kinetics calculations, the typical number of meshes used in the X, Y and Z directions were 76, 68 and 58, respectively, and the time step used was 0.01 seconds. For the reactor boundary conditions, an extrapolated distance of 10 cm to zero flux was used in both the X and Y directions, and 7 cm in the Z direction. The diffusion cell parameters that were input to the DONJON code were generated by using the WIMS code [5]. The main transport calculations were performed using 18 energy groups, and later collapsed into 2 groups for the homogenized cell parameters.

3. Calculation Method of DONJON

In the simulations of NRU, the calculation method of DONJON used a standard fully implicit time integration scheme for determining the time dependent two energy group fluxes (ϕ_1, ϕ_2) and for the six delayed neutron precursor concentrations ($C_1, C_2, ...C_6$). This implicit integration scheme was chosen because it is unconditionally stable. The spatial part was treated with mesh centred finite differences. In the NRU simulation, the delayed photo-neutrons were ignored, and the kinetic parameters for the neutron fractions, β_n, and decay constants, λ_n, of the six delayed neutron groups were taken from standard U235 data (see for example [6]).

Using standard notation, the equations for the time-dependent diffusion of neutrons in a reactor are:

$$[v]^{-1}\frac{\partial}{\partial t}[\Phi] = \nabla.[D]\nabla[\Phi] - [\Sigma][\Phi] + (1-\beta)[\chi_p][\nu\Sigma_f]^T[\Phi] + \sum_{n=1}^{6}[\chi_{dn}]\lambda_n C_n, \text{ and} \quad (1)$$

$$\frac{\partial}{\partial t}[C_n] = \beta_n[\nu\Sigma_f]^T[\Phi] - \lambda_n C_n, \text{ with } n = 1,2,....6. \quad (2)$$

The semi-discrete formulation of the above space-time kinetics equations can be written as:

$$\frac{\partial}{\partial t}[\psi] = [H][\psi], \quad (3)$$

where $[\psi]$ is a vector comprising the fast- and thermal-group fluxes and delayed neutron precursor concentrations at each mesh point of the core.

$$[\psi] = col\{[\phi_1,\phi_2],[C_1],[C_2],[C_3],[C_4],[C_5],[C_6]\} \quad (4)$$

The quantity $[H]$ is a square, sparse matrix with seven bands per energy group, whose entries depend on the specific spatial discretization of the core, on the geometry and on the homogenized cross sections and diffusion coefficients.

The implicit scheme of time integration leads to the system of equations,

$$\left[I - [H]_n \Delta t\right][\psi]^{n+1} = [\psi]^n, \quad (5)$$

where $[\psi]^{n+1}$ is the unknown vector at t_{n+1}, at the end of the time interval and $[\psi]^{n}$ is the known vector at t_n, calculated from the previous time interval.

Also, $[H]_n$ represents the constant value of $[H]$ during this same time interval between t_n and t_{n+1}. This matrix changes from one time interval to the other because of perturbations, such as rod movements and other changes in cross sections during the transient.

The system of equations in (5) is solved at each time interval during the transients, using the Successive Over Relaxation (SOR) iterative scheme. In this scheme, the matrix $[I - [H]_n \Delta t]$ is partitioned into a diagonal matrix $[D]$, a lower triangular matrix $[C_L]$ and an upper triangular matrix $[C_U]$. The solution for $[\psi]$ is obtained by:

$$[D][\psi]^{(m+1),n+1} = \omega\left\{[C_L][\psi]^{(m+1),n+1} + [C_U][\psi]^{(m),n+1} + [\psi]^{n}\right\} + (1-\omega)[D][\psi]^{(m),n+1}, \qquad (6)$$

where the index m in parenthesis indicates the iteration number for space, with the other index n for time. The stationary acceleration parameter ω was kept fixed for all time intervals, and was given the value obtained in the initial static part of the calculation.

The calculation of the dynamic reactivity and other point kinetics parameters, such as the mean neutron lifetime, was performed at each time interval, from the detailed spatial solution $[\psi]^{n+1}$ obtained. The point kinetics parameters were useful in the correct interpretation of the transient behaviour.

4. Simulation of Four Reactor Transients

Simulations were performed for the following four NRU transients to cover different rates of reactivity insertion:

1. Central control rod at site J16 driving out at maximum speed.
2. Off-center control rod at site G06 driving out at maximum speed.
3. U-2 Loop blow-down (voiding of the light water coolant) at site E20.
4. U-1 Loop blow-down (voiding of the light water coolant) at site L08.

In each of the first two transients, the control rod started from the half-inserted position in the reactor core. Simulation of control rod movement was performed by changing the cross sections in the appropriate cells at different time steps for a maximum control rod withdrawal speed of 12.7 cm/s. The first transient was simulated for 1.25 s, and the second for 2.50 s (because the center control rod has a higher reactivity insertion rate than the off-center control rod). The transient time chosen in each case was long enough to provide calculation results for the reactor power to increase by 20% or more. Under these circumstances, the reactor would have been shut down well before then.

In each of the last two transients, the loop contained a string of 6 fresh natural uranium CANDU fuel bundles, and was initially filled with light water coolant. Loop voiding was simulated by changing the cell parameters for the loop from full coolant to no coolant in a linear fashion over the transient period of 1 s.

During the transient at time $t = t_n$, the power generated in kW for a given reactor site I and axial position k, is obtained from the Q factors, the two-group fluxes and the axial height according to:

$$p_{I,k}(t_n) = [(Q_1 * \phi_1(t_n))_{I,k} + (Q_2 * \phi_2(t_n))_{I,k}] * \Delta Z_k \qquad (7)$$

where Q_1 and Q_2 are the 2 group linear heat ratings per unit cell height per unit flux, in kW/cm/unit flux,

$\phi_1(t_n)$ and $\phi_2(t_n)$ are the 2 group cell averaged fluxes, and

ΔZ_k is the cell height in axial position k, in cm.

The assembly power $P_I(t_n)$, at site I, is given by summing the cell powers over all the axial sections at that site:

$$P_I(t_n) = \sum_k P_{I,k}(t_n)$$

At the beginning of each transient, the initial power distribution for the reactor core was calculated, and the total reactor power was normalized to 1 watt. During the transient, the power distribution and the total reactor power increase were re-calculated for each time increment of 0.01 s until the end of transient.

5. Results

The central control rod transient results are given below. Figure 2 shows the total reactor power increase as a function of time. At the end of the transient, the 3D amplitude factor for total power increase was 1.200. Figure 3 shows the ratio of assembly power increase during the transient, i.e. the assembly power at the end of the transient to the power at the beginning of the transient. In this Figure, the powers are normalized to the same total reactor power, and this shows the change in power shape, not the change in absolute power. We see that the maximum change occurs in channel H15, for a ratio of 1.048, and the second highest change occurs in channel H19 for a ratio of 1.030. The power distribution displays a local power peak near Control Rod 16.

Figure 2: Total Power as a function of Time – J16 Transient

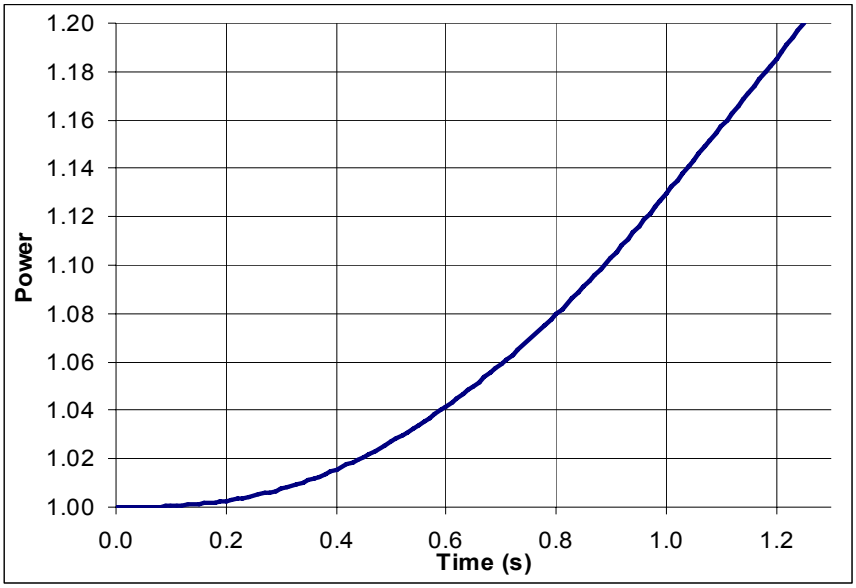

Figure 3: Ratio of assembly power increase normalized to the same total reactor power for the central control rod withdrawal transient

	A	B	C	D	E	F	G	H	J	K	L	M	N	O	P	Q	R	S
0																		
1																		
2																		
3						0.991		0.991		0.991		0.991						
4							0.992				0.991							
5						0.992												
6					0.992													
7				0.993				0.994		0.994		0.993						
8			0.993				0.995				0.994		0.991					
9		0.993								0.996		0.994		0.992				
10					0.996		0.998		0.999		0.997							
11		0.994						1.002		1.010						0.992		
12			0.995		0.998		1.013										0.993	
13				0.997		1.011		1.008		1.007		1.007		0.996		0.993		
14					1.001				1.016		1.006				0.996		0.994	
15		0.996		0.998		1.004		1.048				1.013		0.997				
16					1.000								1.000				0.994	
17				0.999		1.016		1.018		1.016				0.998				
18			0.998		1.000						1.008		1.001				0.995	
19		0.997		0.999		1.004		1.030		1.027		1.003		0.998				
20									1.009		1.016		1.001					
21				0.998				1.007		1.006						0.996		
22							1.011		1.014									
23		0.996				1.000				1.019						0.996		
24			0.996				1.000		1.007						0.997			
25				0.997				1.000				0.999						
26					0.997				0.999		0.998							
27						0.997								0.997				
28					0.996		0.997				0.997							
29								0.997		0.997								
30																		
31																		
32																		

Table 1: Axial Variation of the power ratios before and after the transient

Plane	Axial Ht. (cm)	J14 unperturbed t=0.0 s	J14 perturbed t=1.25 s	J14 Power Ratio	H17 unperturbed t=0.0 s	H17 perturbed t=1.25 s	H17 Power Ratio
1	175.0 ~ 182.0	0.000E+00	0.000E+00	0.000E+00	0.000E+00	0.000E+00	0.000
2	162.5 ~ 175.0	0.000E+00	0.000E+00	0.000E+00	0.000E+00	0.000E+00	0.000
3	150.0 ~ 162.5	0.000E+00	0.000E+00	0.000E+00	0.000E+00	0.000E+00	0.000
4	137.0 ~ 150.0	0.000E+00	0.000E+00	0.000E+00	0.000E+00	0.000E+00	0.000
5	125.0 ~ 137.0	4.456E-04	4.443E-04	9.971E-01	4.361E-04	4.356E-04	0.999
6	112.5 ~ 125.0	5.176E-04	5.166E-04	9.982E-01	5.206E-04	5.206E-04	1.000
7	100.0 ~ 112.5	5.813E-04	5.812E-04	9.998E-01	5.933E-04	5.943E-04	1.002
8	87.5 ~ 100.0	5.728E-04	5.740E-04	1.002E+00	5.895E-04	5.920E-04	1.004
9	75.0 ~ 87.5	6.182E-04	6.216E-04	1.006E+00	6.411E-04	6.461E-04	1.008
10	62.5 ~ 75.0	6.613E-04	6.680E-04	1.010E+00	6.907E-04	6.995E-04	1.013
11	50.0 ~ 62.5	7.039E-04	7.156E-04	1.017E+00	7.405E-04	7.549E-04	1.019
12	38.0 ~ 50.0	7.207E-04	7.395E-04	1.026E+00	7.621E-04	7.843E-04	1.029
13	25.0 ~ 38.0	7.578E-04	7.889E-04	1.041E+00	7.991E-04	8.344E-04	1.044
14	12.5 ~ 25.0	8.051E-04	8.590E-04	1.067E+00	8.518E-04	9.102E-04	1.069
15	0 ~ 12.5	8.628E-04	9.385E-04	1.088E+00	9.148E-04	9.942E-04	1.087
16	-12.5 ~ 0	9.401E-04	9.890E-04	1.052E+00	9.943E-04	1.048E-03	1.054
17	-25.0 ~ -12.5	9.860E-04	1.016E-03	1.031E+00	1.041E-03	1.076E-03	1.033
18	-38.0 ~ -25.0	1.009E-03	1.027E-03	1.018E+00	1.065E-03	1.086E-03	1.020
19	-50.0 ~ -38.0	1.021E-03	1.031E-03	1.010E+00	1.082E-03	1.095E-03	1.012
20	-62.5 ~ -50.0	1.045E-03	1.050E-03	1.004E+00	1.106E-03	1.112E-03	1.006
21	-75.0 ~ -62.5	1.020E-03	1.020E-03	1.000E+00	1.074E-03	1.076E-03	1.001
22	-87.5 ~ -75.0	9.827E-04	9.796E-04	9.969E-01	1.030E-03	1.028E-03	0.998
23	-100.0 ~ -87.5	9.316E-04	9.264E-04	9.945E-01	9.705E-04	9.663E-04	0.996
24	-112.5 ~ -100.0	9.616E-04	9.545E-04	9.927E-01	9.947E-04	9.885E-04	0.994
25	-125.0 ~ -112.5	8.661E-04	8.586E-04	9.914E-01	8.838E-04	8.771E-04	0.992
26	-137.0 ~ -125.0	7.510E-04	7.439E-04	9.906E-01	7.461E-04	7.398E-04	0.992
27	-150.0 ~ -137.0	0.000E+00	0.000E+00	0.000E+00	0.000E+00	0.000E+00	0.000
28	-162.5 ~ -150.0	0.000E+00	0.000E+00	0.000E+00	0.000E+00	0.000E+00	0.000
29	-175.0 ~ -162.5	0.000E+00	0.000E+00	0.000E+00	0.000E+00	0.000E+00	0.000
30	-182.0 ~ -175.0	0.000E+00	0.000E+00	0.000E+00	0.000E+00	0.000E+00	0.000
		0.01776	**0.01804**	**1.016**	**0.01853**	**0.01886**	**1.018**

However, sufficiently far away from the J16 rod (~ 4 lattice pitches away), the distribution is relatively unchanged.

The transient power distribution also exhibits an axial variation, and the maximum change occurs in plane 15 of fuel channel J14. The detailed axial power distributions of this assembly and H17 at the end of the transient are given in Table 1. The maximum final/initial point power ratio was 1.088 at site J14, axial plane 15. The point power increase for this mesh was therefore 1.088 * 1.200 = 1.305.

The DONJON simulation results for the three remaining transients are shown in Table 2. Results for the second transient for the off-center control rod withdrawal from site G06 are given below. The initial position of the rod was with the bottom of the absorber at the reactor mid-plane, and the rod was then moved out at the maximum allowed speed of 12.7 cm/s for 2.50 s. The 3D amplitude factor for total power increase at the end of the transient was 1.372. The maximum final/initial normalized point power ratio was 1.259

at site G04, axial plane 14. The point power increase for this mesh was therefore 1.259 * 1.372 = 1.727.

In the third transient of voiding the coolant from the E20 loop site, the site was filled with a string of 6 fresh natural uranium bundles. The static reactivity worth of the coolant was 3.324 mk. The voiding occurred by changing in a linear fashion from parameters representing full coolant to voided coolant over a period of 1 s. The 3D amplitude factor for total power increase after the transient was 1.471. The maximum final/initial normalized point power ratio was 1.141 at site D21, axial plane 13. The point power increase was therefore 1.471*1.141 = 1.679.

Table 2: Summary of DONJON Calculation Results for NRU.

Case	Site	Transient Type	Rate of Reactivity* Insertion (mk/s)	Time of Transient Analyzed (s)	Total Reactor Power Increase Col. 6	Maximum Change in Flux Shape Factor (Location) Col. 7	Mesh Peak Power Ratio (Location) Col. 6 x Col. 7
1	J16	Center control rod moving up at max. speed from half inserted position	1.301	1.25	1.200	1.088 (Site J14, Plane 15)	**1.305** (Site J14, Plane 15)
2	G06	Off-center control rod moving up at max. speed from half inserted position	0.775	2.50	1.372	1.259 (Site G04, Plane 14)	**1.727** (Site G04, Plane 14)
3	E20	Loop voiding	3.324	1.00	1.471	1.141 (Site D21, Plane 15)	**1.679** (Site D21, Plane 15)
4	L08	Loop voiding	3.046	1.00	1.419	1.089 (Site M03, Plane 16)	**1.545** (Site M03, Plane 16)

*Reactivity (in mk) = $(1-\frac{1}{k})\times 1000$, where k is the neutron multiplication factor.

The fourth transient was similar to the third, modeling the voiding of the coolant from the L08 loop site. In the model, the site was filled with a string of 6 fresh natural uranium bundles, and the static reactivity worth of the coolant was 3.046 mk. The voiding occurred by changing in a linear fashion from parameters representing full coolant to voided coolant over a period of 1 s. The 3D amplitude factor for total power increase at the end of the transient was 1.419. The maximum final/initial normalized point power ratio was 1.089 at site M03, axial plane 16. The maximum point power increase was therefore 1.419*1.089 = 1.545.

6. Comparison with Other Codes

Previously, kinetic analysis of NRU has been performed using a point kinetic model, based on the assumption that the NRU reactor is relatively tightly coupled. To test the validity of this assumption, the DONJON results were compared with those from the point kinetics calculations of the thermal hydraulic code CATHENA [7]. For this comparison, the same kinetics parameters for the six delayed neutron groups, and the same neutron lifetime of 1.835 ms, were used as in DONJON. Also, the CATHENA calculations were performed with all the trips and thermal hydraulic feedback disabled. The results of the comparison for the four transients are summarized in Table 3. The total reactor power increase at the end of each transient from DONJON agreed with the point kinetics model in CATHENA to within ~2.5%, which is within the calculational uncertainty. The results show that the power increase ratios for CATHENA are slightly higher than the 3D DONJON results, indicating that the point kinetics method is conservative relative to the DONJON 3D kinetics calculations in predicting the total reactor power increases for these transients.

Table 3: Total Reactor Power Increase for Each Transient

	Transient Description	**DONJON (3D Kinetics) col.3**	**CATHENA (Point-kinetics) col.4**	**% Difference (col.4-col.3)/col.3**
1	Central control rod withdrawal at J16	1.200	1.230	+2.5%
2	Off-Center control rod withdrawal at G06	1.372	1.404	+2.3%
3	E20 loop voiding	1.471	1.497	+1.8%
4	L08 loop voiding	1.419	1.447	+1.6%

The flux shape change factors for the four transients, column 7 of Table 2, were checked using the DONJON *static* calculation, and agreed within 1%. Thus, the flux shape change factor for a transient in the NRU reactor can be determined by *static* calculations from other codes.

The above DONJON simulation results are also being checked against another well established reactor kinetics code, NESTLE [8], to confirm the predicted kinetic behavior.

7. Summary

In summary, the DONJON code, initially designed for CANDU power reactor analysis, has been applied to analyze transients in the highly heterogeneous NRU research reactor. Results were used to confirm previous NRU kinetics analysis methods, i.e. there was good agreement (within 2.5 %) between point-kinetics simulations of the reactor power increases following postulated reactivity transients in NRU and DONJON 3D kinetics modeling. For the NRU reactor, the peak point power during a transient can be determined by multiplying the total reactor power amplitude increase by the flux shape change factor, which can be calculated from static calculations.

References:

[1] D. T. Nishimura, "Summary of Loops in Chalk River NRX and NRU Reactors", AECL Report, AECL-6980, December (1980).

[2] E. Varin, J. Koclas and R. Roy, "Application of the DONJON Reactor Code for Regulating System Simulations", Proceedings of the 19th CNS Simulation Symposium, Hamilton, Ontario, Canada, Oct. 16-17, (1995).

[3] J. Mao and J. Koclas , "The Analytic Nodal Method for CANDU Reactor Three-Dimensional Space-Time Kinetics Calculations", Proceedings, 21st Annual Conference of the Canadian Nuclear Society, June (2000).

[4] J. Koclas, B. Forget, "Implementation of a Full P1 Method in the Diffusion Code DONJON/NDF", Physor 2004, Chicago, Illinois, USA, April 25-29, (2004).

[5] J.D. Irish and S.R. Douglas, "Validation of WIMS-IST", Proceedings of the 23rd Annual Conference of the Canadian Nuclear Society, Toronto, Canada, June (2002).

[6] Reactor Physics Constants, Argonne National Laboratory, ANL 5800, July (1963).

[7] T.G. Beuthe and J.B. Hedley, "Preliminary Investigation of the Solution of Sparse Matrices in CATHENA", Proceedings of the 20th CNS Simulation Symposium, Niagara-on- the-Lake, Ontario, Canada, Sept. 7-9 (1997).

[8] P.J. Turinsky, et al, "NESTLE-Computer Code Abstract", Nuclear Science and Engineering, **120**, 72 (1995).